Optics Communications 300 (2013) 269–273

Contents lists available at SciVerse ScienceDirect

Optics Communications

journal homepage: www.elsevier.com/locate/optcom

Direct integration of aspherical microlens on vertical-cavity surface emitting laser emitting surface for beam shaping

Qi-Song Li [a,b], Li-Jie Wang [c], Zhen-Nan Tian [a], Xiao-Feng Lin [b], Tong Jiang [b], Jun Zhang [b], Xing Zhang [c], Ji-Hong Zhao [b,**], Ai-Wu Li [b], Li Qin [c,*]

[a] College of Physics, Jilin University, 2699 Qianjin Street, Changchun 130012, China
[b] State Key Laboratory on Integrated Optoelectronics, College of Electronic Science and Engineering, Jilin University, 2699 Qianjin Street, Changchun 130012, China
[c] Key Laboratory of Excited State Processes, Changchun Institute of Optics, Fine Mechanics and Physics, Changchun 130033, China

ARTICLE INFO

Article history:
Received 12 May 2012
Received in revised form
7 February 2013
Accepted 22 February 2013
Available online 29 March 2013

Keywords:
VCSEL
Aspherical microlens
Femtosecond laser direct writing
Divergence angle

ABSTRACT

The aspherical microlens used for beam shaping of vertical-cavity surface emitting lasers (VCSELs) was designed and fabricated. The microlens designed as needed was directly fabricated and integrated in one step on the emitting surface of a VCSEL by femtosecond laser direct writing (FsLDW). By the microlens' shaping the beam quality of VCSELs can be remarkably improved, especially the reduction of the divergence angle. The experiment results agree with the numerical modeling results. After integrating aspherical microlenses the far-field divergence angle of the VCSEL was reduced from 18.16° to 0.83°. This novel technique has great potential in the field of miniature and low power integrated optical system.

1. Introduction

The vertical-cavity surface-emitting laser (VCSEL) has been proved to be a low-cost light source with attractive properties such as facile fabrication of two-dimensional arrays, high-efficiency and easy integration [1–5]. These features, together with its high speed modulation [6], have given it a wide range of applications in, for example, short-distance parallel fiber-optic interconnects [7], ultrafast all-optical switching [8], and chaotic sources [9,10]. However, some disadvantages in its beam properties bring a negative influence on its practical uses. A main disadvantage is the large divergence angle [11,12], which is caused by VCSELs' short cavity-length. So the beam shaping of VCSELs needs to be implemented for practical applications. Up to now, the traditional means of laser beam shaping are utilizing the diffractive micro-optical elements [13–15] like Fresnel lens or the refractive micro-optical elements [16–18] including various spherical microlenses. In these methods, an independent micro-optical element was positioned in a certain place away from the laser emitting surface. And there were some problems to be resolved, such as complex adjustment process, instability and difficulties for integration. Additionally, both the substrate for supporting microlens and the air-gap between the laser emitting window and the microlens could lead to reflection and refraction which might further influences the performances. Therefore, approaches of one-step fabrication and integration directly on emitting surface have been attracting great efforts [19,20]. Especially, a GaAs-based refractive microlens was directly integrated onto the surface of the emitting window by the wet-etching technology in our previous work [20]. Owning to complex processing procedures and lack of ability of arbitrarily designed fabrication, the previously reported approach was not very good and the divergence angle was only reduced to 7°. In consideration of above problems, the aspherical microlens, which attracted more efforts than the spherical microlens did [21], was directly written onto emitting surface of the VCSEL to reduce the divergence angle of the laser beam via femtosecond laser direct writing.

Femtosecond laser direct writing technology (FsLDW) [22–35] has been recently considered as a promising approach to conveniently integrate arbitrary three-dimensional (3D) micro-optical devices towards integrated optical circuits. Attributing to its micro- and nano-scale-high accuracy and material compatibility [23,32], FsLDW provides the possibility of fabricating complicated surfaces on a variety of substrates. Various micro-optical devices, such as micro logarithmic axicon lenses [24], Dammann grating [28], and multilevel phase-type fractal zone plates [33] have been realized.

In this paper, the aspherical microlens was fabricated by femtosecond laser direct writing based on two-photon polymerization of resins [34] and directly integrated in one step onto emitting surface

* Corresponding author. Tel.: +13756180032.
** Corresponding author.
E-mail addresses: zhaojihong@jlu.edu.cn (J.-H. Zhao), qinl@ciomp.ac.cn, qinlicloud@sina.com (L. Qin).

0030-4018/$ - see front matter © 2013 Elsevier B.V. All rights reserved.
http://dx.doi.org/10.1016/j.optcom.2013.02.063

of the VCSEL. Due to the capability of pinpoint writing with nano-scale accuracy arbitrary profile, as-need aspherical microlenses could be constructed and simultaneously positioned onto the emitting surface, which resulted into convenient system integration and was difficult to be achieved by any other microfabrication technologies [36–41]. Meanwhile, the reflection and refraction could be eliminated in contrast with the common pattern by the microlens that was placed on the substrate of cover glass. What's more, relative location of the elements including the collimation and distance could be easily controlled by our approach for improved and stabilized beam shaping performances. As a result, reduction of divergence angle was further improved by an order of magnitude compared with the GaAs-microlens approach (from 7° to 0.83°).

2. Experiments

A schematic diagram of the FsLDW micro/nano-fabrication system is shown in Fig. 1. A Ti-sapphire femtosecond laser (from Tsunami, Spectra Physics) was used. It generated laser with wavelength at 780 nm mode-locked with a duration of 120 fs at a repetition rate of 80 MHz, which was tightly focused into the resin by a high numerical aperture (60×, NA=1.42, oil immersion) objective lens. The processing laser power was optimized to be ~6 mW which was measured before the objective lens. A lens was first designed with a CAD (Computer Aided Design) program and transformed into data of point coordinates. Controlled by the fabrication program that had read the data, a rotating mirror set along with a 1-D piezo stage where the sample was located made the focal spot move three-dimensionally relatively to the sample resist and the smallest pace of the motion is as accurate as 1 nm. The scan step that the femtosecond laser moved on polymerization of resins is usually chosen to be 100 nm in our experiments for an overall consideration of both micro-fabrication's quality and elapsed time. Because of the opaqueness of substrate (emitting window of VCSEL), the detecting light irradiated from bottom to top could be reflected and propagated along the same path into CCD. Then the VCSEL's emitting window would be visually monitored on the computer display screen by the CCD so that the microlens could be fabricated accurately at the position of the emitting window. In our experiment SU-8 films were prepared by spin-coating on the surface of an unpackaged VCSEL, since the wire-lead of VCSELs would prevent the fabrication of the aspherical microlens on the emitting surface after packaged. After soft-bake steps at 65 °C for 10 min and at 95 °C for 40 min, the solvent was evaporated and a film with thickness of ~100 μm was obtained. The photoinitiator generated spatial distribution acid under the irradiation of femtosecond laser resulting photo-crosslinking. In the process of the post-exposure bake at 95 °C for 10 min, the latent structure was converted into a cross-linked solid skeleton by the chain propagation of the crosslinking process. Then, the film was developed in the SU-8 developer (1-methoxy-2-propylacetate) about 30 min, leaving the expected structures on the VCSEL's emitting surface for testing. In our work, the emitting wavelength of VCSEL was 850 nm, the operating voltage was 2.39 V and the current was 80 mA.

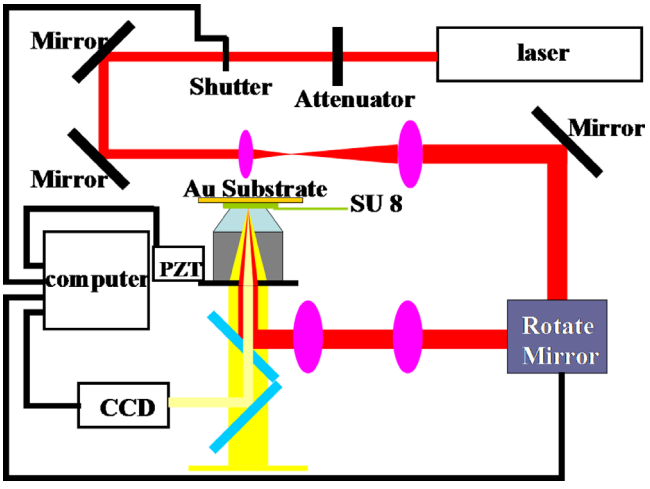

Fig. 1. A schematic diagram of the femtosecond microfabrication system of opaque substrate.

Microlenses were made of commercial photo-resist SU-8 2075 photopolymer. This photo-resist has been widely used due to its high transmittance of wavelengths from the visible to near infrared wavelengths, low volume shrinkage, good mechanical properties (Young's modulus of 4 GPa and biaxial modulus of elasticity of 5.2 GPa), high thermal stability (degradation temperature of 380 °C), and good adhesion on metal. Usually, below 380 °C, the change of performance caused by thermal expansion and thermal-optic effect is nearly ignorable. In consideration of the change of temperatures range from 50 °C to 100 °C, the thermal expansion coefficient of SU-8 is approximately 52 ppm/°C and the changed size of SU-8-based microlens is less than 260 nm for the diameter of 100 μm. At the same time, the thermal-optic coefficient of the SU-8 is about -1.8×10^{-4}/°C and the change of the refractive index would not be larger than 0.01, which also helps to assure the stability of SU-8-based microdevices. All of these make SU-8 resist be a good material for polymer micro-optical components and the divergence angle of VSCELs will be insensitive to temperature through the beam shaping of the SU-8-based microlens.

3. Result and discussion

For a lens with aspherical surface, parallel light rays that passed through the central region of the lens focus to the same position as light rays that passed through the edges of the lens do. An aspherical lens eliminates the spherical aberration and reduces other optical aberrations. So an aspherical lens may bring a better result when it is used for beam shaping of the VCSEL. To verify this, the optical field distribution and the beam profile of VCSEL were simulated by the Rsoft software for the two conditions: without and with the integration of the aspherical microlens. As indicated in Fig. 2, the Gaussian beam with a beam waist of 5 μm was chosen as the light source to analyze whether existence of the aspherical microlens would effectively reduce the divergence angle of VCSELs effectively. As shown in Fig. 2(a) and (b), the distribution of optical field indicated that the diameter of the Gaussian beam decreased greatly after integrating the aspherical microlens. In Fig. 2(c) and (d), the intensity distribution at the position of $z=100$ μm and 300 μm were exhibited, respectively. Herein, simulated positions were chosen to be in a short distance to the emitting window for better observation, which is enough for the qualitative demonstration of the microlens' beam shaping ability. Thus, it was experimentally proved that the radius of beam was decreased by the integrated-microlens. Furthermore, the ideal far-field divergence angle could be calculated through the change of beam waist at different positions.

Hyperbolical microlenses were firstly fabricated on opaque substrate, for example, Au film on the cover glass, to optimize the processing parameters. In Fig. 3(a) and (c), the hyperboloidal microlens fabricated FsLDW from SU-8 on opaque films was characterized by a field emission scanning electron microscopy (SEM, JSM-7500F, JEOL) after sputter-coating Au film with a thickness of ~10 nm using an auto fine coater (at a current of

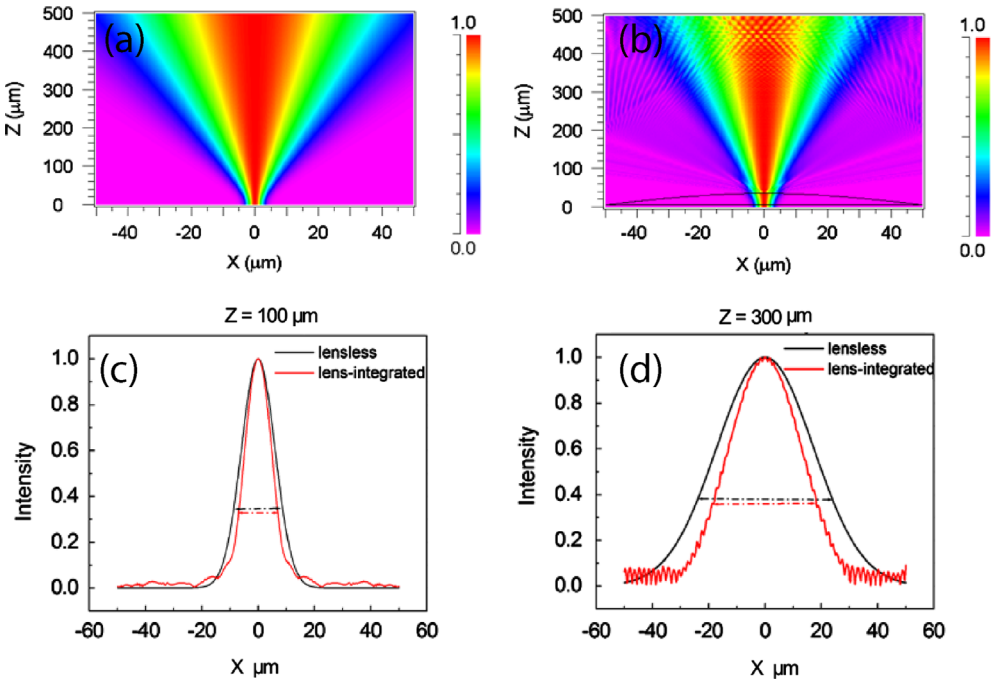

Fig. 2. (a) and (b) The optical field without and with an aspherical microlens integrated, utilizing the Rsoft software for simulation of the Gaussian beam. (c) The beam profile at $z=100$ μm of without and with microlens integrated. (d) The beam profile at $z=300$ μm of without and with microlens integrated.

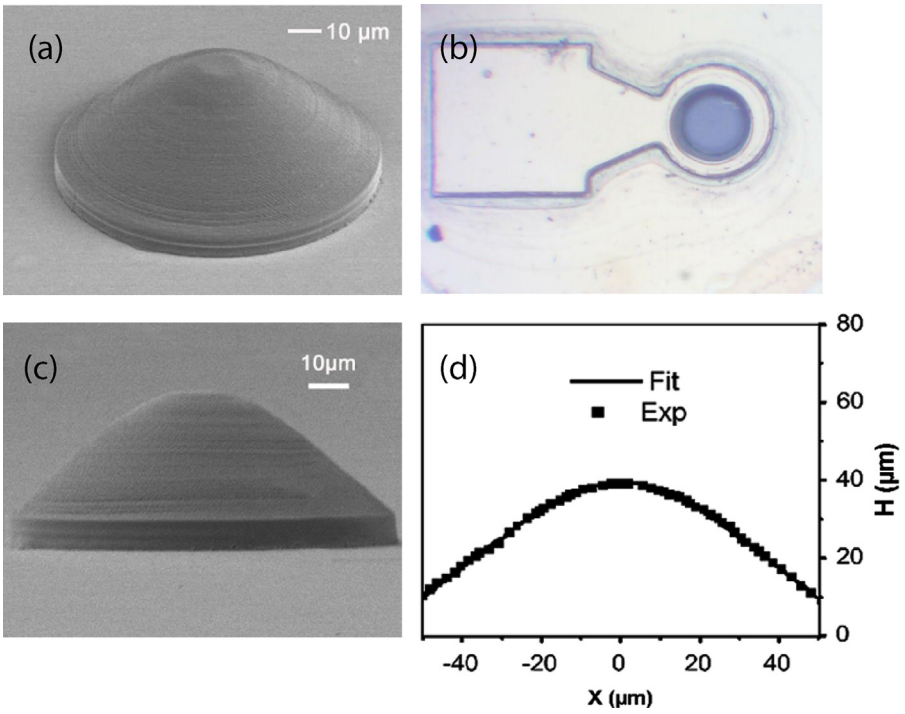

Fig. 3. (a) SEM image of a hyperboloidal microlens with a 10-μm pedestal on the Au substrate. (b) The optical microscope images after integating an aspherical microlens on the VCSEL surface. (c) Lateral-view SEM image of a single microlens on the Au substrate. (d) The measured profile (the square symbol) and the theoretical curve (the line).

20 mA for 60 s, JFC-1600, JEOL). The microlens with a diameter of 100 μm and a height of 30 μm was placed on a pedestal with a height of 10 μm. The size of the microlens could be designed arbitrarily according to the divergence angle of VCSELs. The optimal femtosecond laser power was about 6 mW and the exposure time was chosen as 100 ms on consideration of both the reducation of the fabrication time and enough 3D shape and surface qualities. After optimization of processing parameters using an opaque substrate, we then directly fabricated and integrated the microlens onto the VCSEL's emitting surface which was not wire-leaded just as Fig. 3(b). When the laser pulse energy was stabilized and processing parameters were fully optimized, the average surface roughness of SU-8-based microlens could be less than 2.5 nm for voxel–voxel distance of 100 nm. During the FsLDW of microlens directly on the emitting surface of VCSELs, the femtosecond laser did not cause any damage to the laser emitting window because of low average power (6 mw) and single pulse energy (several PJ), and the power of the emergent laser beam

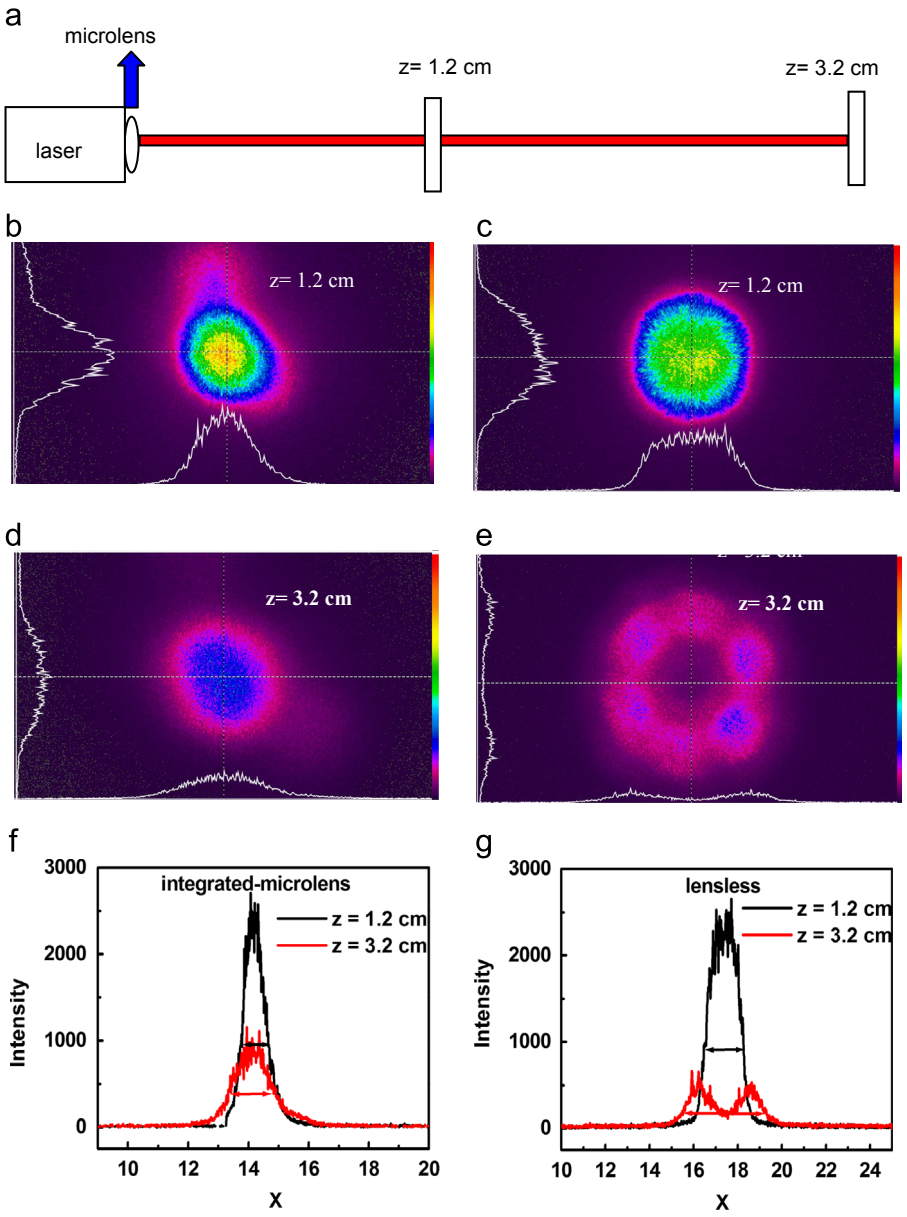

Fig. 4. (a) Setup for measuring the size of spots at different positions. (b) and (d) The spots at $z=1.2$ cm and 3.2 cm after intergrating microlens. (c) and (e) The spots at $z=1.2$ cm and 3.2 cm before integrating microlens. (f) The intensity distribution of the beam spots in (b) and (d). (g) The intensity distribution of beam spots in (c) and (e).

only decreased a little and the insertion loss is about 10% by measuring the emergent power of integrated-microlens compared with the situation without integrated-microlens. It may prevent the Fresnel reflection occurring at the surface of microlens and reduce the insertion loss of the microlens by improving the surface roughness of the microlens and depositing an antireflection coating on the surface of the microlens. In Fig. 3(c), the lateral view of the microlens showed that the profile of lens was a hyperbolically aspheric surface, in accordance with the relation of $r^2=(n^2-1)\times h^2+2\times(n-1)\times f\times h$, where r is the radius of the microlens, h is the height, f is the focal length and n is the refractive index of SU-8. The formula can be considered as an equation of hyperbola when r and h are regarded as independent variables. As in Fig. 3(d), the measured line of the lens profile was found to be perfectly consistent with the theoretical curves of the aforementioned equation which was simulated with the Origin software. The relative error was less than 1%, far smaller than that in other approaches, e.g. 8% in thermal reflow.

The simple measuring setup of divergence angle was shown in Fig. 4(a). Usually, there are three methods in the measurement of the laser divergence angle: The Focus Length Methods (ISO standard), Far-Field Wide Angle Method and Far-Field Two Point Method [42]. Each is valid under different operating conditions. In our work, because of the large divergence angle of VCSELs, the Far-Field Two Point Method was adopted instead of The Focus Length Methods (ISO standard). And In the case of the approximation, the two other methods are equal to The Focus Length Methods (ISO standard). Radius and shape of laser beam at different position in the far-field region were compared to calculate the divergence angle as well as the effect of aspherical lens by Eq. (1)

$$\theta=\arctan\left(20\times\frac{R_1-R_2}{d}\right) \tag{1}$$

where R_1 and R_2 are the radii of two spots at different positions on the CCD, and d is the distance between the two spots. In the measurement of divergence angle, the size of spot was minified

twenty times owing to the restriction of the receiving range of CCD. So in Eq. (1), an extra factor 20 should be added to the right part of Eq. (1). The spot shape of the lensless VCSEL at $Z_1=1.2$ cm and $Z_2=3.2$ cm were shown in Fig. 4(c) and (e), respectively. When $Z_2=3.2$ cm, higher-order mode appeared in Fig. 4(e). After beam shaping of the integrated-microlens the topography was improved as shown in Fig. 4(b) and (d) for positions of $Z_1=1.2$ cm and $Z_2=3.2$ cm positions, respectively. Especially in Fig. 4(d), modes of laser were greatly ameliorated after the integrated-microlens. Because of the far-field distance, the variation of beam waist was close to the size variation of spots. We would only consider the sizes of spots rather than the beam waist in favor of the far-field divergence angle. Fig. 4(f) and (g) showed the intensity distribution of the spots at different positions, also the spot sizes could be obtained. The diameter of the spots were 604 μm at $Z_1=1.2$ cm position and 1260 μm at $Z_2=3.2$ cm position for the condition of lensless VCSEL system. By applying Eq. (1), the divergence angle of the lensless laser was calculated to be 18.16°. Similarly, the diameter of the spots was 346 μm at the position of $Z_1=1.2$ cm and 375 μm at the position of $Z_2=3.2$ cm after the microlens had been integrated. The divergence angle of the semiconductor VCSEL integrated with a microlens was reduced to 0.83°. Here, although experimental measurements are done at much longer distances ($Z_1=1.2$ cm and $Z_2=3.2$ cm) for conveniently testing in the far-field region of the VCSEL, the experiment results agree with the Rsoft simulation in the trend. In addition, considering an actual working 850 nm VCSEL, the temperature increment (from ~30 °C to ~80 °C) would not exceed 50 °C. For the temperatures change from 30 °C to 80 °C, the beam shaping ability of the SU-8-based microlens (defined as the divergence angle's reduction) was estimated to change by only ~1 mrad based on SU-8's thermal-optic and thermal expansion coefficients.

4. Conclusion

In conclusion, we have successfully fabricated the aspherical microlens directly on the surface of a semiconductor VCSEL for a convenient integration by FsLDW approach. An integrated constructions of micro-optical elements with 3D arbitrarily designed profile, aspherical microlenses here, was realized by this technology, and significant improvement on the mode and divergence angle of the laser beam was obtained by the direct integration of SU-8 aspherical microlenses. The divergence angle of the semiconductor VCSEL integrated with the microlens was reduced from 18.16° to 0.83°. Importantly, the fabrication-integration in one step was endowed with drastically simplified procedures and high-precision position. It provides a novel application with great potential in fields such as polymer micro optics, laser beam shaping, miniaturized integrated optical systems, etc.

Acknowledgements

The authors gratefully acknowledge support from NSFC (Grant Nos. 90923037, 61137001 and 61008035).

References

[1] J.L. Jewell, J.P. Harbison, A. Scherer, Y.H. Lee, L.T. Florez, IEEE Journal of Quantum Electronics 27 (1991) 1332.
[2] K. Iga, In Vertical-Cavity Surface-Emitting Laser Devices, Springer, Berlin, Germany1.
[3] S. Viciani, M. Gabrysch, F. Marin, F.M.D. Sopra, M. Moser, K.H. Gulden, Optics Communication 206 (2002) 89.
[4] M. Grabherr, M. Miller, R. Jager, R. Michalzik, U. Martin, H.J. Unold, K.J. Ebeling, IEEE Journal on Selected Topics in Quantum Electronics 5 (1999) 495.
[5] F. Koyama, Journal of Lightwave Technology 24 (2006) 4502.
[6] G. Sialm, D. Lenz, D. Erni, G.L. Bona, C. Kromer, M.X. Jungo, T. Morf, F. Ellinger, H. Jäckel, IEEE Journal of Lightwave Technology 23 (2005) 2318.
[7] J. Jahns, F. Sauer, B. Tell, K.F. Brown-Goebeler, A.Y. Feldblum, C.R. Nijander, W.P. Townsend, Optics Communication 109 (1994) 328.
[8] B.T. Zhang, D.W. Snoke, A.P. Heberle, Optics Communication 284 (2011) 3011.
[9] S.Y. Xiang, W. Pan, B. Luo, L.S. Yan, X.H. Zou, N. Jiang, L. Yang, H.N. Zhu, Optics Communication 284 (2011) 5758.
[10] Y. Xiao, T. Deng, Z.M. Wu, J.G. Wu, X.D. Lin, X. Tang, L.B. Zeng, G.Q. Xia, Optics Communication 285 (2012) 1442.
[11] Y. Zhang, Y.Q. Ning, Y. Wang, J.J. Cui, G.Y. Liu, X. Zhang, Z.F. Wang, T. Li, L. Qin, Y.F. Sun, Y. Liu, L.J. Wang, Optics Communication 283 (2010) 2719.
[12] A.J. Liu, M.X. Xing, H.W. Qu, W. Chen, W.J. Zhou, Applied Physics Letters 94 (2009) 191105.
[13] Y. Lin, J.H. Hu, K.N. Wu, Optics Communication 282 (2009) 3210.
[14] N. Passillya, M. Fromagera, L. Mechinb, C. Guntherb, S. Eimerb, T. Mohammed-Brahimc, K. Ait-Ameura, Optics Communication 241 (2004) 465.
[15] H. Martinsson, J. Bengtsson, M. Ghisoni, A. Larsson, IEEE Photonics Technology Letters 11 (1999) 503.
[16] O. Blum, S.P. Kilcoyne, M.E. Warren, T.C. Du, K.L. Lear, R.P.Jr. Schneider, R.F. Carson, G. Robinson, F.H. Peters, IEEE Electronics Letters 31 (1995) 44.
[17] S. Eitel, S.J. Fancey, H.P. Gauggel, K.H. Gulden, W. Bächtold Senior Member, IEEE, M.R. Taghizadeh, IEEE Photonics Technology Letters 12 (2000) 459.
[18] T.R.M. Sales, Optical Engineering 42 (2003) 3084.
[19] Y.Q. Fu, N.K. Ann Bryan, Optics Express 10 (2002) 413.
[20] Z.f. Wang, Y.Q. Ning, T. Li, J.j. Cui, Y. Zhang, G.Y. Liu, X.Z, L. Qin, Y. Liu, L.J. Wang, IEEE Photonics Technology Letters 21 (2009) 239.
[21] D. Wu, Q.D. Chen, L.G. Niu, J. Jiao, H. Xia, J.F. Song, H.B. Sun, IEEE Photonics Technology Letters 21 (2009) 1535.
[22] A. Baum, S.D. Nicola, S. Abdalah, K. Al-Naimee, A. Geltrude, M. Locatelli, R. Meucci, W. Perrie, P.J. Scully, A. Taranu, F.T. Arecchi, Optics Communication 284 (2011) 2771.
[23] Y.L. Sun, W.F. Dong, R.Z. Yang, X. Meng, L. Zhang, Q.D. Chen, H.B. Sun, Angewandte Chemie 124 (2012) 1590.
[24] X.F. Lin, Q.D. Chen, L.G. Niu, T. Jiang, W.Q. Wang, H.B. Sun, Journal of Lightwave Technology 28 (2010) 1256.
[25] C.H. Tu, Z.C. Huang, S.G. Zhang, M.L. Hu, Q.Y. Wang, E.B. Li, Y.N. Li, F.Y. Lu, Optics Communication 284 (2011) 455.
[26] Y.L. Zhang, Q.D. Chen, H. Xia, H.B. Sun, Nano Today 5 (2010) 435.
[27] L.L. Qiao, F. He, C. Wang, Y. Liao, Y. Cheng, K.J. Sugioka, K. Midorikawa, C. Pan, X.B. Wei, Optics Communication 284 (2011) 2988.
[28] Q.D. Chen, X.F. Lin, L.G. Niu, D. Wu, W.Q. Wang, H.B. Sun, Optics Letters 33 (2008) 2559.
[29] K.L.N. Deepak, R. Kuladeep, D. Narayana Rao, Optics Communication 284 (2011) 3070.
[30] K. Takada, D. Wu, Q.D. Chen, S. Shoji, H. Xia, S. Kawata, H.B. Sun, Optics Letters 34 (2009) 566.
[31] L. Li, R.R. Gattass, E. Gershgoren, H. Hwang, J.T. Fourkas, Science 324 (2009) 910.
[32] H. Xia, J. Wang, Y. Tian, Q.D. Chen, X.B. Du, Y.L. Zhang, Y. He, H.B. Sun, Advanced Materials 22 (2010) 3204.
[33] D. Wu, S.Z. Wu, L.G. Niu, Q.D. Chen, R. Wang, J.F. Song, H.H. Fang, H.B. Sun, Applied Physics Letters 97 (2010) 0371109.
[34] D. Wu, Q.D. Chen, L.G. Niu, J. Wang, R. Wang, H. Xia, H.B. Sun, Lab on a Chip 9 (2009) 2391.
[35] X.Z. Dong, Q. Ya, X.Z. Sheng, Z.Y. Li, Z.S. Zhao, X.M. Duan, Applied Physics Letters 92 (2008) 231103.
[36] J. Albero1, L. Nieradko, C. Gorecki, H. Ottevaere, V. Gomez, H. Thienpont, J. Pietarinen, B. Päivänranta, N. Passilly, Optics Express 17 (2009) 6283.
[37] R. Guo, S.Z. Xiao, X.M. Zhai, J.W. Li, A.D. Xia, W.H. Huang, Optics Express 14 (2006) 810.
[38] Madanagopal V. Kunnavakkam, F.M. Houlihan, M. Schlax, J.A. Liddle, P. Kolodner, Applied Physics Letters 82 (2003) 1152.
[39] C.S. Lima, M.H. Hongb, A. Senthil Kumara, M. Rahmana, X.D. Liuc, International Journal of Machine Tools and Manufacture 46 (2006) 552.
[40] H.T. Hsieh, V. Lin, J.L. Hsieh, G.D. John Su, Optics Communication 284 (2011) 5225.
[41] H. Schmitt, M. Rommel, A.J. Bauer, L. Frey, A. Bich, M. Eisner, R. Voelkel, M. Hornung, Microelectronic Engineering. 87 (2010) 1074.
[42] BeamGage User Guide, 2011 Ophir-Spiricon, LLC.